

Optical patterning of magnetic domains and defects in ferromagnetic liquid crystal colloids

A. H. ... (1.2,3a)
¹D. ... P ... s ... C ... ad, B ... d ... C ... ad 80309, USA
²Ma ... a s Sc ... c a d E ... P ... a ... D ... a ... E ... c ... ca ... C ... a d E ... E ...
³R ... ab ... a d S ... s a ab E ... I ... s ... Na ... a R ... ab E ... Lab ... a ... a d U ... s ...
C ... ad, B ... d ... C ... ad 80309, USA

(Received 18 July 2015; accepted 3 August 2015; published online 20 August 2015)

A promising approach in designing composite materials with an unusual physical behavior combines solid nanocrystals and orientationally ordered soft matter materials. Such composites can not only inherit properties of their constituents but also can exhibit emergent behaviors such as ferromagnetic ordering of colloidal metal nanoparticles, forming magnetic monopole domains, when dispersed in a nematic liquid crystal. Here, we demonstrate the optical patterning of domains, crystals, and topological defects in such ferromagnetic liquid crystal colloids, which allow for aligning their response to magnetic fields. Ordering reveals the nature of the defects in terms of magnetic moments, which is different from non-polar nematics and ferromagnets alike. © 2015 AIP Publishing LLC. [<http://dx.doi.org/10.1063/1.4928552>]

Liquid crystal (LC) colloids attract considerable attention of scientists in order to benefit from the richness of their

500 mg of 5CB, 95 μl of pentacene (5CB, Chengde
 Yonghua Materials Co. Ltd.) and 5 μl of
 a benzene-concentrated beam 1205 LC (Beam Co.). Non-
 isomerizing FLCs (pencil 2) were used for
 optical defect patterning. 100 μl of pure
 5CB and hexamethylbenzene were used for the
 preparation of the FLC. Silane-PEG capped magnetic
 nanoparticles were added to the LC. 5 μl of
 ethanol was added to 15 μl of the LC mixture to bring
 the isotropic phase, followed by adding 15 μl of 0.1%
 magnetic nanoparticles in ethanol. The samples were
 kept at 90 °C for 3 h to allow the ethanol to
 evaporate and the nanoparticles to be dispersed,
 and then rapidly cooled to the nematic phase of the
 mixture. The FLC was centrifuged at 2000 rpm
 for 5 min to remove residual aggregates. The
 final composition contained only well-dispersed
 nanoparticles. The volume fraction of magnetic
 nanoparticles in the LC varied from 0.05 to 0.1%,
 as determined based on absorbance and magnetic
 ionization. Nanoparticles exhibited spontaneous
 alignment in large-area faceted or hexagonal
 magnetic domains along $\mathbf{n}(\mathbf{r})$, as confirmed by
 polarized ion-dependent absorbance¹⁶ and probing
 of their dielectric properties of magnetic
 ferroelectric nanoparticles in the LC mixture
 (up to 20 mT) exhibiting a facile reorientation
 below 1 mT. Homeotropic glass cells in the
 FLC and M pointing in one of the two in-parallel
 directions along the vertical far-field direction
 \mathbf{n}_0 were prepared using 1- or 0.17-mm thick glass plates
 coated with an aqueous solution of 0.1%
 N,N-dimethyl-N-ocadecyl-3-aminopropyl-
 trimethylammonium chloride (DMOAP, Acros
 Organics) via dip-coating. The cell gap thickness
 of 30 μm or 60 μm was achieved by
 spacers between the glass plates at their edges
 with UV-curable optical adhesive (NOA-65,
 Norland Products) or epoxy coating of
 corresponding diameters. Cell filling was
 done at room temperature using capillary
 action. FLC cells exhibited spontaneous
 formation of random magnetic domains
 of lateral dimensions typically comparable
 or some have larger than the cell thickness
 and depend on the initial ion field of 10–35 mT
 (Refs. 4 and 16) (Fig. 1)

the orientation of $\mathbf{M}(\mathbf{r})$ is opposite in-plane orientation, as depicted in Fig. 3(b), although $\mathbf{n}(\mathbf{r})$ also contains (Fig. 3(a)) because half-in-integer defects are allowed in the $\mathbf{n}(\mathbf{r})$ line field but not in the $\mathbf{M}(\mathbf{r})$ vector field.

Although, in principle, simultaneous patterning of both $\mathbf{M}(\mathbf{r})$ and $\mathbf{n}(\mathbf{r})$ can be achieved by combining the approaches described above, it is interesting to note the evolution of domains in $\mathbf{M}(\mathbf{r})$ when only the direction is patterned (Fig. 4). The $\mathbf{M}(\mathbf{r})$ in thin magnetic domains in the patterned region follows the patterned $\mathbf{n}(\mathbf{r})$ in thin magnetic domains and behaves differently (splitting of opposite domains) in the in-plane domain. A applied magnetic field, the pol domain nature of the FLCC in explaining the topologically required all connecting the half-integer defect lines in $\mathbf{n}(\mathbf{r})$, causing a complete pattern of domains and all defects in explaining them, which follow the evolution in time and strongly depend on both the direction and strength of \mathbf{B} . In explaining, the width of all defects in thin regions of different $\mathbf{n}(\mathbf{r})$ of even larger than has in regions of uniform direction (Fig. 4). To consider the nature of magnetic in-plane domain in the FLCC, evidenced dark field microcopy observations have real both locations and orientation of individual nanoparticles (polarized video S1)²² a zero field and then \mathbf{B} a different orientation, electric field, the domains of opposite \mathbf{M} . Unlike in conventional magnetic systems, here magnetic domains are typically

separated by the so-called Bloch or Néel walls⁸ in combination of local eddy current deformations of $\mathbf{M}(\mathbf{r})$, magnetic in the in-plane domain of the FLCC, is not needed, so has the accompanying nature. This is because $\mathbf{M}(\mathbf{r})$ and $\mathbf{n}(\mathbf{r})$ are strongly coupled, so has the eddy current deformations of $\mathbf{M}(\mathbf{r})$ between the domains would be coupled in terms of the corresponding elastic deformations of $\mathbf{n}(\mathbf{r})$. Indeed, the domain walls in the FLCC have uniform direction and the $\mathbf{M}(\mathbf{r})$ so has here is not associated elastic free energy density of each wall. A applied field, the in-plane domain walls can be partially deprived of nanoparticles (polarized video S1) and ranging in width from the average spacing between individual nanoparticles of $\sim 1\mu\text{m}$, as determined by colloidal interactions between nanoparticles with different oriented dipole moments of the neighboring domains of opposite $\mathbf{M} \parallel \mathbf{n}_0$. When $\mathbf{n}(\mathbf{r}) \parallel \mathbf{M}(\mathbf{r})$ in thin domains is different, this in explaining further altered by the energetic cost of elastic deformations (Fig. 4). Although the domain walls defects in the FLCC are similar in $\mathbf{M}(\mathbf{r})$, different from the eddy current Bloch or Néel walls commonly observed in magnetic systems,⁸ one-, two-, and three-dimensional defects can also form in the chiral conformation of the FLCC, in which different $\mathbf{n}(\mathbf{r}) \parallel \mathbf{M}(\mathbf{r})$ directions are promoted by the chiral nature of the LC host.¹⁶

Unlike conventional LCs, which exhibit a reponse to magnetic field has much less, faster than the reponse to electric field, the FLCCs are sensitive to a $\approx 1\text{mT}$ field and exhibit polar response. Although either only magnetically uniform or random pol domain FLCCs applied electric field previously,^{4,7,16} our work demonstrates that the magnetic domains can be patterned on macroscopic length scales in many different ways, allowing for engineering the macroscopic response of such materials to magnetic field. Since this patterning is achieved in a reconfigurable fashion, allowing for in-plane illumination, ordering, and manipulation of macroscopic reduction of material composition in the natural properties and facile pre-defined response to weak external stimuli. Beyond the potential practical aspects, the experimental framework has developed material one could hope the polar nature of ordering in such materials is one property of topological defects and solutions. In addition to small-molecule liquid crystalline hosts of magnetic nanoparticles, the FLCC ordering can potentially be patterned in polymeric, elastomeric, and other materials.

To conclude, we have demonstrated the optical patterning of magnetic domains and defects in the FLCCs. Because of the facile magnetic patterning in the reconfigurable domain polarity and elastic deformation patterning, our experimental framework may lead to realizing structures and compositions well beyond the ones presented in this letter. The introduction of chirality and particle-like entities can enable magnetic control of complex optical phenomena such as nematicon formation and deflection,¹⁷ electric reconnection,^{18,19} noncontact manipulation of defects,^{20,21} etc. Moreover, polymer or elastomeric networks in the FLCCs may yield novel mechanical behavior of the engineering of solid systems such as programmable strain bias and electric mechanical actuation.^{12,14}

We acknowledge discussions with N. Clark, W. Ganne, M. Keller, P. Ackerman, A. Marin, T. Whi, e,

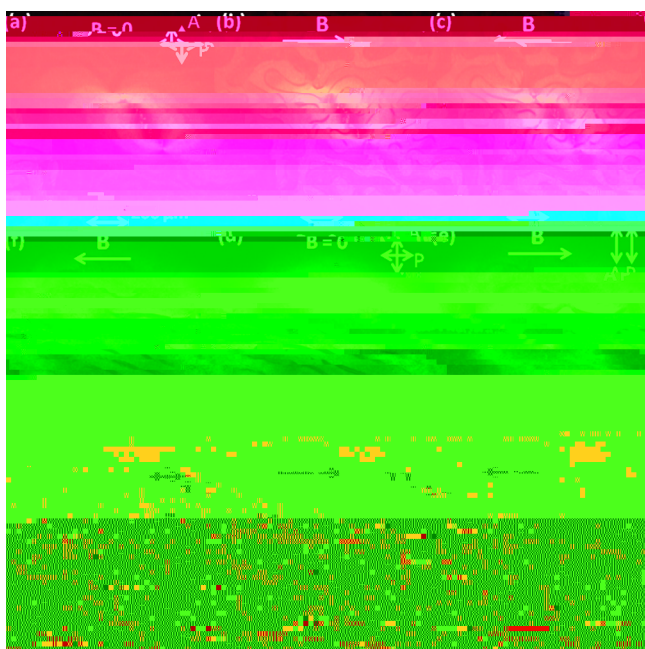


FIG. 4. POM images of FLCCs in which patterned defects. (a) A micrograph of the structure corresponding to $\mathbf{n}(\mathbf{r})$ shown in Fig. 3, in which the walls in $\mathbf{M}(\mathbf{r})$ are visible as a bright jiggling line. An in-plane \mathbf{B} along opposite directions marked in (b) and (c), which complements domains in an in-parallel non-uniform $\mathbf{M}(\mathbf{r})$. (d) (i) POM images of the FLCC cell in a dichroic ion pair. The in-plane dichroic ion and other \mathbf{M} -all defects separate magnetic domains are clearly visible. Polarizing micrographs (a) (d) and (g) were taken in horizontal polarizer (P) and analyzer (A), while the responses were obtained in parallel P and A, as shown in the double arrows. The red-light illumination used to obtain POM micrographs shown in (a) (f) and yellow-light illumination used in (g) (i) present in ended changes of surface boundary conditions through photoalignment during imaging. The comparison of micrographs (d) (f) and (g) (i), which were taken $\approx 10\text{min}$ after (d) (f), demonstrates the evolution of domains in time.

and Y. Zhang. This research was supported by the NSF grant DMR-1420736. A.J.H. and I.I.S. acknowledge the AFSOR faculty fellowship and the hospitality of the Air Force Research Laboratory during the time when his work was under preparation for publication.

¹P. Politin, H. Sarkis, T. C. L. Beach, and D. A. Wei, *Science* **275**, 1770 (1997).

²C. P. Lapointe, T. G. Mason, and I. I. Smal'kh, *Science* **326**, 1083 (2009).

³Q. Li, Y. Cui, D. Gardner, X. Li, S. He, and I. I. Smal'kh, *Nano Letters* **10**, 1347 (2010).

⁴A. Mereljić, D. Lijak, M. Drofenik, and M. Čopić, *Nature* **504**, 237 (2013).

⁵Q. Li, Y. Yan, and I. I. Smal'kh, *Nano Letters* **14**, 4071 (2014).

⁶Q. Li, B. Senk, J. Tang, T. Lee, J. Qian, S. He, and I. I. Smal'kh, *Physical Review Letters* **109**, 088301 (2012).

⁷A. Mereljić, N. Omerman, D. Lijak, and M. Čopić, *Soft Matter* **10**, 9065 (2014).

⁸P. M. Chaikin and T. C. L. Beach, *Physics of Crystals and Liquid Crystals* (Cambridge University Press, Cambridge, 1995).

⁹M. Schadt, H. Seiberle, and A. Scherzer, *Nature* **381**, 212 (1996).

¹⁰K. Ichimura, *Chemical Reviews* **100**, 1847 (2000).

¹¹A. Marinone, H. C. Mireles, and I. I. Smal'kh, *Proceedings of the National Academy of Sciences U.S.A.* **108**, 20891 (2011).

¹²T. H. Ware, M. E. McConne, J. J. Wie, V. P. Tondiglia, and T. J. Whie, *Science* **347**, 982 (2015).

¹³U. A. Hroch, S. V. Serak, N. V. Tabiryan, and T. J. Bunning, *Advanced Materials* **19**, 3244 (2007).

¹⁴M. E. McConne, A. Marinone, V. P. Tondiglia, K. M. Lee, D. Langle, I. I. Smal'kh, and T. J. Whie, *Advanced Materials* **25**, 5880 (2013).

¹⁵D. Lijak and M. Drofenik, *Croatian Journal of Chemistry* **12**, 5174 (2012).

¹⁶